Supporting Information

Epitaxy: Programmable Atom Equivalents *Versus* Atoms

Mary X. Wang,[&,†,‡] Soyoung E. Seo,[&,§,‡] Paul A. Gabrys,[∥] Dagny Fleischman,[⊗] Byeongdu Lee,[#] Youngeun Kim,[⊥,‡] Harry A. Atwater,[⊗] Robert J. Macfarlane,[*,∥] and Chad A. Mirkin[*,†,§,⊥,‡]

Table S1. DNA sequences used for functionalizing AuNPs and the substrate. Thiolated strands (X-SH) that had a 3' propyl thiol-modifier were functionalized onto AuNPs. These strands consisted of two of six ethylene glycol units (denoted as $(EG6)_2$) close to 3' propyl thiol to increase the flexibility of the DNA. HS-A DNA strands used for nanoparticles and the substrate are identical, and so are Linker A strands.

DNA Type	Sequence (5'-3')
Nanoparticles	
HS-A	TCA ACT ATT CCT ACC TAC $(EG6)_2$-SH
HS-B	TCC ACT CAT ACT CAG CAA $(EG6)_2$-SH
Linker A	GTA GGT AGG AAT AGT TGA A TTT AGT CAC GAC GAG TCA TT A TTT AGT CAC GAC GAG TCA TT A TTCCTT
Linker B	TTG CTG AGT ATG AGT GGA A TTT AGT CAC GAC GAG TCA TT A TTT AGT CAC GAC GAG TCA TT A AAGGAA
Duplexer	AAT GAC TCG TCG TGA CTA AA
Substrate	
HS-A	TCA ACT ATT CCT ACC TAC $(EG6)_2$-SH
Linker A	GTA GGT AGG AAT AGT TGA A TTT AGT CAC GAC GAG TCA TT A TTT AGT CAC GAC GAG TCA TT A TTCCTT
Duplexer	AAT GAC TCG TCG TGA CTA AA

Oligonucleotides were synthesized on an ABI 394 (Applied Biosystems) automated oligonucleotide synthesizer using standard phosphoramidite chemistry on controlled pore glass (CPG) beads. Phosphoramidite reagents and CPG beads (GlenUny Support) were purchased from Glen Research (Sterling, VA). After synthesis, oligonucleotides were deprotected using a fast deprotection method, where 1 μmole of synthesized oligonucleotides was mixed with 1 mL of a 1:1 mixture (*v*) of 40% aqueous methylamine and 30% ammonium hydroxide solution, then was allowed to sit at 25 °C for 2 hours. After deprotection, the solvent containing the DNA was evaporated with nitrogen, and the sample was filtered through a 0.2 μm pore syringe filter to remove the CPG beads and impurities. To remove failure strands from the success strands, the DNA was purified using reverse-phase high performance liquid chromatography (Varian RP-HPLC) on an Agilent C18 column. After the purification step *via* RP-HPLC, the DNA was lyophilized overnight. To cleave the acid-labile 4,4'-dimethoxytrityl (DMT) protecting group off the DNA, 1-2 mL of 20% acetic acid was added per 1-2 μmole columns of dry DNA. After the solution was allowed to sit for approximately 1 hour, 2 mL of water and 3-4 mL of ethyl acetate were added to remove hydrophobic DMT groups and extract the purified DNA from the solution. All oligonucleotides were characterized and confirmed by matrix-assisted laser desorption/ionization time-of

flight (MALDI-TOF) mass spectrometry to ensure that all molecular weights corresponded to the theoretical masses. The MALDI-TOF mass spectrometry matrix was prepared by dissolving 30 mg of 3-hydroxypicolinic acid (Fluka) in 1 mL of a 1:1 MeCN:H_2O solution and mixed with 10 mg of ammonium citrate dibasic (Sigma-Aldrich). 1.5 µL of diluted oligonucleotide was aliquoted and mixed with 1.5 µL of this matrix on a steel plate to crystallize prior to MALDI-TOF analysis. The absorbance of oligonucleotides was measured on a Cary 5000 UV-Vis-NIR spectrophotometer (Agilent) using calculated extinction coefficients from Integrated DNA Technologies (IDT) website.

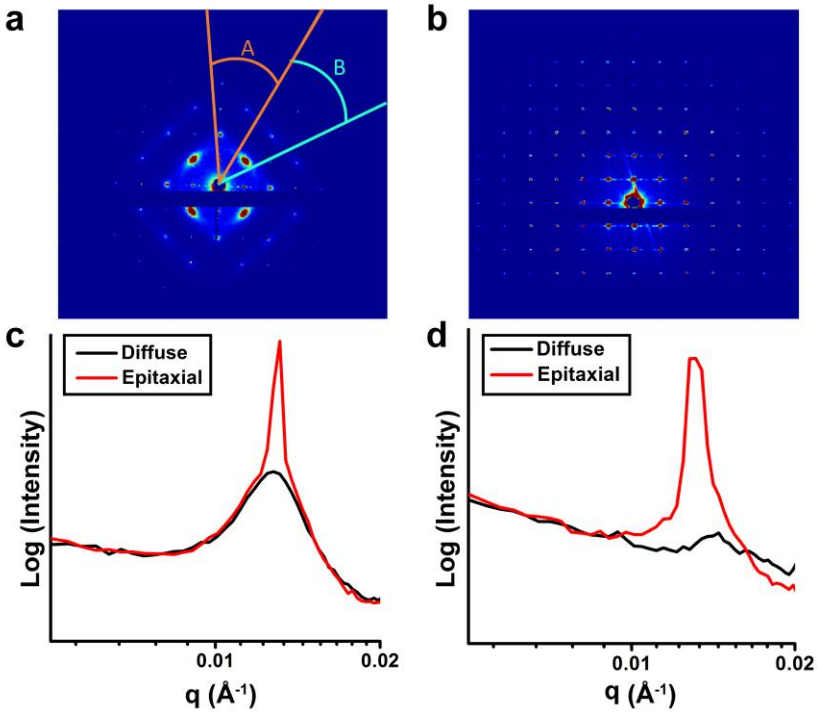

Figure S1: Analysis of SAXS Data. a) Sector averaging to determine degree of epitaxy. The background signal from the diffuse ring is determined from azimuthally averaging arc A. The signal corresponding to the epitaxial NPs is determined from the azimuthally averaging arc B. b) SAXS scattering pattern of a blank patterned substrate. The scattering intensity comes from the gold posts on the pattern. The 1D averaged data from the 2D pattern is shown for the 10-layer thin film samples assembled at c) 25 °C and d) (T_m-4) °C and annealed.

Since epitaxial PAEs are oriented in the bcc [100] direction, their in-plane scattering produces strong signal intensity present as a spot. On the other hand, PAEs that are not epitaxial are randomly oriented in the z-direction, even if they possess bcc symmetry, and their scattering produces a circular ring. Therefore, by comparing the integrated signal intensity from the (110) peak produced by scattering of the

epitaxial PAEs to that of the diffuse ring produced by scattering from the non-oriented PAEs, we can determine the degree of epitaxy. To do this, the center and axis of each SAXS 2D scattering pattern were aligned so that each sample is averaged in the same way (Figure S1a). The background signal from the diffuse ring is determined by azimuthally averaging the 2D scattering pattern over arc A and then fitting the peak using a Voigt profile to get $I_{arc\ A,peak}$. Azimuthally averaging over arc B gives the signal intensity from a combination of 1) PAEs epitaxial with the pattern, 2) the pattern itself (Figures 1 middle and S1b), and 3) the background signal. These 1D data (examples given in Figure S1c and d) obtained for the region corresponding to the bcc (110) peak (Figure 1) were then fit to a Voigt profile, giving $I_{arc\ B,(110)peak}$. The relative degree of epitaxy was then calculated from the ratio of signal from the bcc (110) peak and the corresponding background signal according to equation S1. For each sample, the relative contribution from the lithographically defined pattern remains the same, since the signal for the diffraction peak that overlaps with the region of interest, the (110), is entirely encompassed by arc B for all diffraction patterns.

Equation (**S1**)

$$X_A = \frac{\int I_{arcB,(110)peak} - \int I_{arc\ A,peak}}{\int I_{arcB,(110)peak}}$$

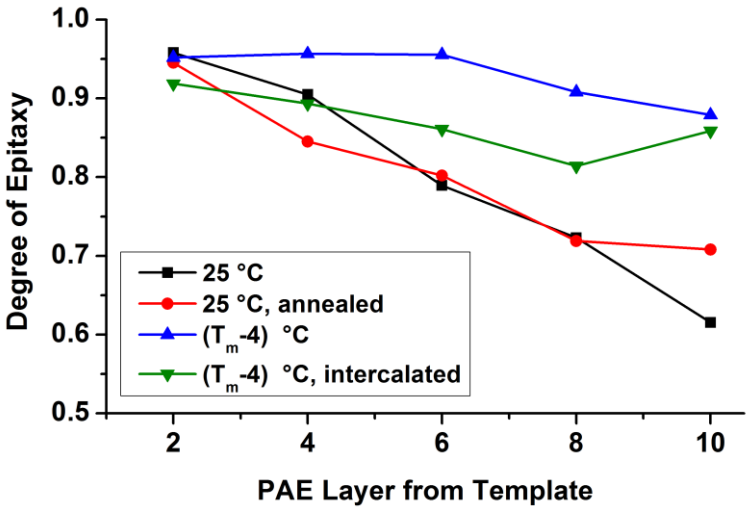

Figure S2: Quantitative analysis of FIB-SEM cross-section. Degree of epitaxy for 10-layer thin films as a function of layer distance from the template, calculated from analysis shown in Figure S5.

Table S2. Mean height and roughness for films of varying layer number grown using different deposition conditions.

	Layer #	Mean Height (nm)	Roughness (nm)	Roughness (nm)
1. 25 °C deposition			Arithmetic Average	Root Mean Squared
	2	130.56	28.46	34.34
	5	311.49	38.46	47.91
	10	775.95	63.87	82.66
2. 25 °C deposition, annealed at (T_m-2) °C				
	5	321.78	46.96	58.82
	10	883.43	79.58	100.09
3. (T_m-4) °C deposition, annealed at (T_m-2) °C				
	2	97.22	20.47	25.76
	5	170.38	36.44	47.52
	10	257.56	29.80	40.31
4. (T_m-4) °C deposition, annealed at (T_m-2) °C, and intercalated				
	2	87.36	23.99	30.42
	10	220.86	46.35	66.95
Unpatterned substrate				
	5	226.34	40.93	53.60

Table S3. Growth Conditions for Templated DNA-NP Superlattice Thin Films.

Condition **1**	Thin films were grown at 25 °C up to 2, 5, and 10 layers
Condition **2**	Thin films were grown to their full thickness at 25 °C, followed by annealing at (T_m-2) °C for 15 minutes in Buffer A. Annealing temperatures varied depending on layer number. Typically, 2-layer thin films were annealed at (T_m-6) °C, and 5- and 10-layer thin films were annealed at (T_m-2) °C due to melting temperature depression observed for thin films.
Condition **3**	The first 2 layers were grown at 25 °C, in which the sample was then annealed at (T_m-2) °C. For third and fourth layers, substrates were immersed in particle solutions at (T_m-6) °C and annealed at (T_m-4) °C. For the rest of the layers, the thin films were grown at (T_m-4) °C and annealed at (T_m-2) °C.
Condition **4**	The growth protocol was same as condition **3**, with the addition of a two hour incubation step in 80 μM intercalator after each annealing step to ensure complete intercalation.

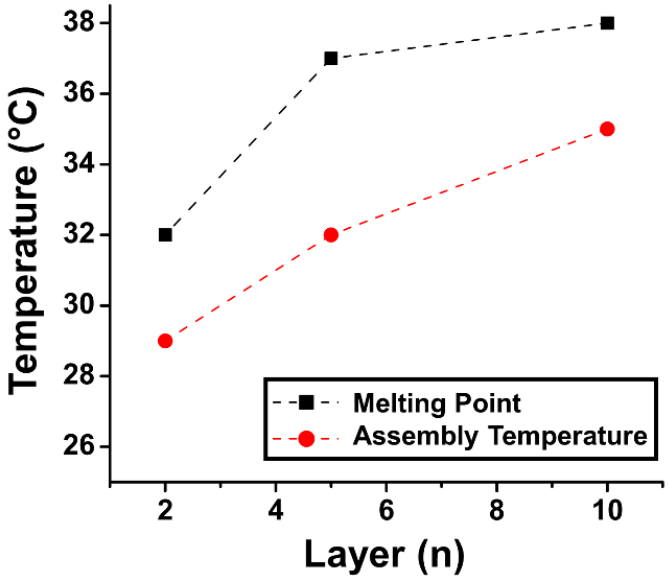

Figure S3: Melting point depression of the templated thin film superlattice as a function of nanoparticle layer number, as determined by SAXS.

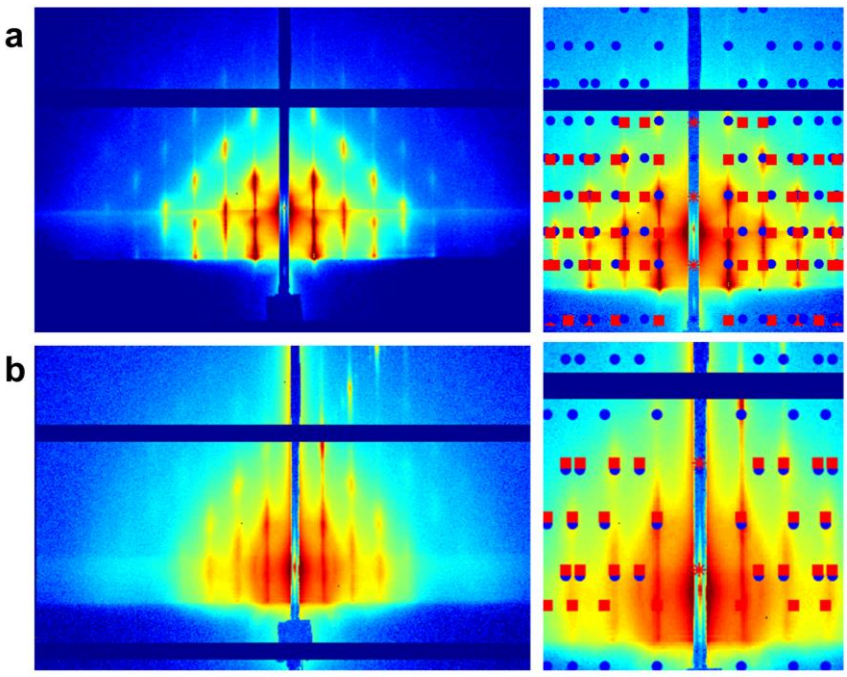

Figure S4: GISAXS of a) 5-layer and b) 10-layer thin films grown at equilibrium conditions. On the right hand side, the scattering patterns were indexed to bcc crystals with (100) orientation corresponding to space group I4/mmm (#139). The higher order peaks evident in the scattering patterns are indicative of long-range order. The high levels of diffuse scattering in the 10-layer film are hypothesized to be due to the thickness of the film, making it difficult for X-ray penetration.

Scheme S1: Demonstration of FIB-SEM cut in different plane orientations.

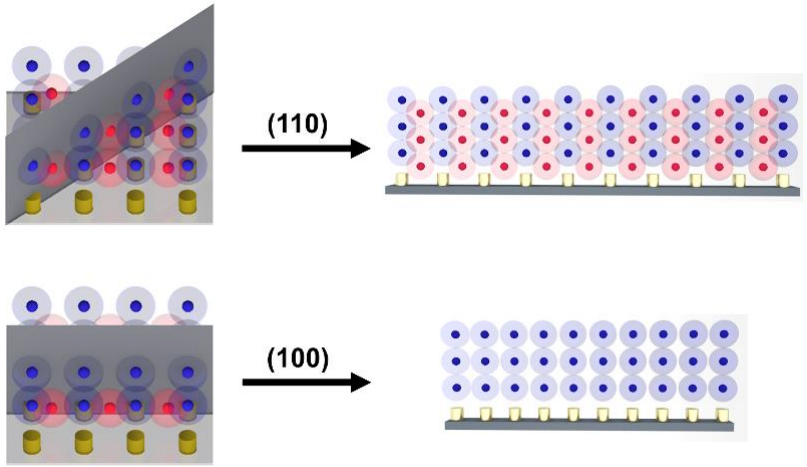

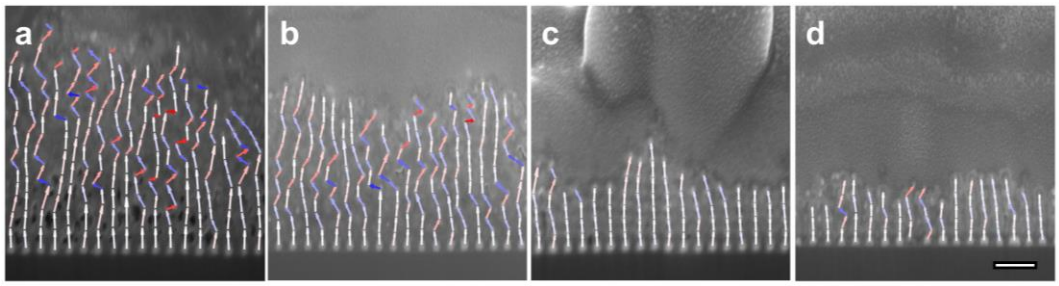

Figure S5: Degree of epitaxy analysis for FIB-SEM cross-sections of 10-layer films grown at a) 25 °C, b) 25 °C and annealed, c) (T_m-4) °C and annealed, and d) (T_m-4) °C, annealed, and intercalated. Scale bar is 200 nm.

Photoshop and Matlab were used to track the positions of internal PAEs relative to the positions of the templated posts. After correcting for tilt, vectors were calculated between adjacent particles in the [001] direction and plotted atop the cross-section of the SEM image. Perfectly epitaxial superlattices would display vectors completely vertical from the posts up throughout the layers; this direction was taken to be 0° (and displayed as white arrows on the overlaid image). Any deviation in z-direction was calculated in terms of degrees where the limits are therefore -90 to 90° (with arrows becoming increasingly blue or red, respectively, as they deviate); note that this vector exists as the projection onto the plane of the cross-section, not as a 3D vector. The first row of vectors was then aggregated and the standard deviation (σ) of their angles was calculated using Matlab. If the vectors were all vertically aligned, *i.e.* the superlattices were perfectly epitaxial, $\sigma = 0$. However, if the vectors were completely random, *i.e.* the superlattices were completely disordered, the maximum standard deviation for this system would be $= \sqrt{((-90 - 90)^2/4)} = 90$. Therefore, to calculate X_A or "Degree of Epitaxy" for that row of vectors such that 1 is perfect epitaxy and 0 is completely disordered, $X_A = (90 - \sigma)/90$. This process was repeated for each row of vectors in the superlattices and plotted in Figure S2. These data corroborate the SAXS results on effects of deposition protocol on epitaxy. While SAXS data provides an averaged information on degree of epitaxy, the analysis on FIB-SEM highlights the waning force of epitaxy the template exhibits over the PAEs as a function of layer number. PAEs within the bulk crystal are more tightly bound and networked with neighboring particles, limiting their vibrational motion. PAEs near the surface of the thin film have fewer neighboring particles, thus have many near-equilibrium positions to easily oscillate between. This

indicates the importance of annealing each layer so that as few defects as possible in the surface layer exist upon the deposition of the subsequent layer to avoid trapping defects in the bulk crystal.

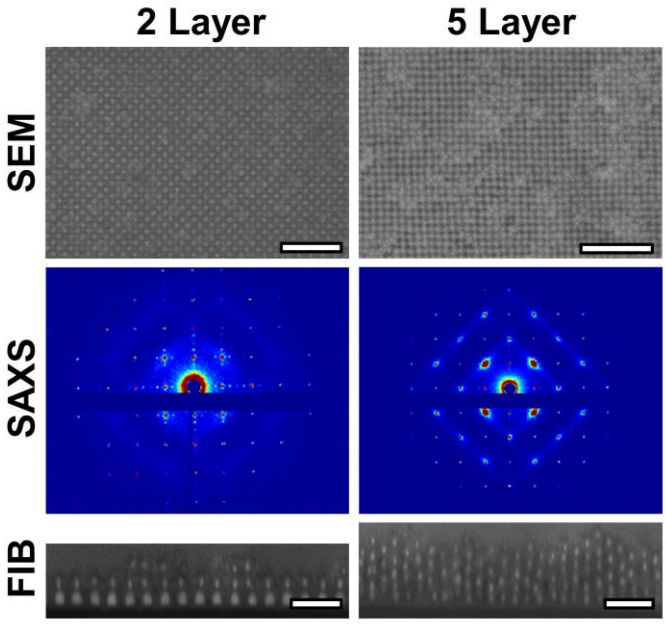

Figure S6: Epitaxial growth of DNA-functionalized nanoparticle thin films at 2 and 5 layers is observed when they are assembled at (T_m-4) °C and annealed. SEM, SAXS, and FIB-SEM show crystalline, epitaxial thin films at 10 layers of nanoparticles. Scale bars for SEM and FIB-SEM are 500 nm and 200 nm, respectively.

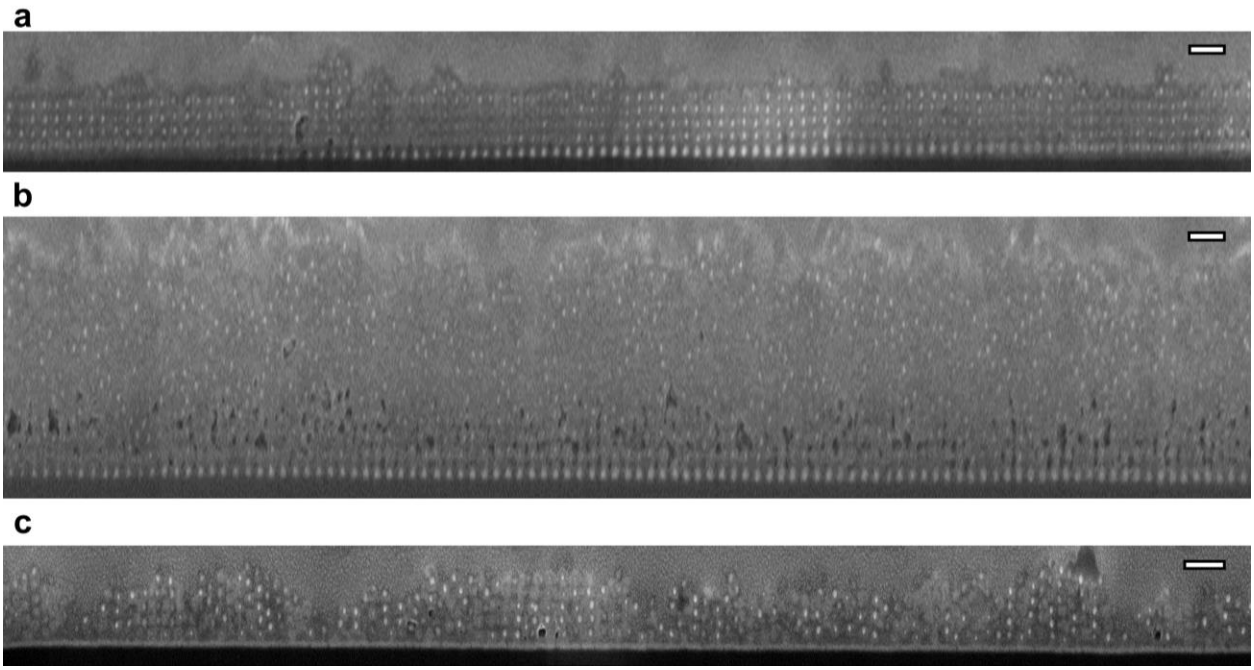

Figure S7: FIB-SEM cross-sections of a) 10-layer film grown on a patterned substrate at (T_m-4) °C, b) 10-layer film grown on a patterned substrate at 25 °C, and c) a 5-layer film assembled on an unpatterned substrate and annealed at (T_m-2) °C. Scale bars are 200 nm.

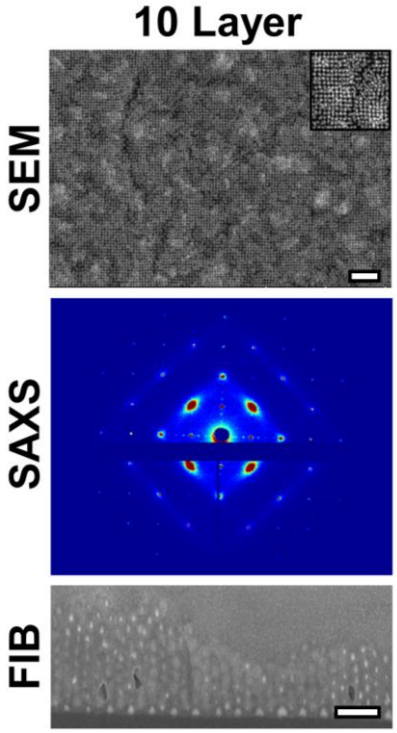

Figure S8: Intercalated 10-layer thin film presenting roughened surface morphology (SEM) and defect propagation along the z-axis (FIB-SEM). SAXS was used to determine the degree of epitaxy (X_A = 0.65). Scale bars for SEM and FIB-SEM are 500 nm and 200 nm, respectively.

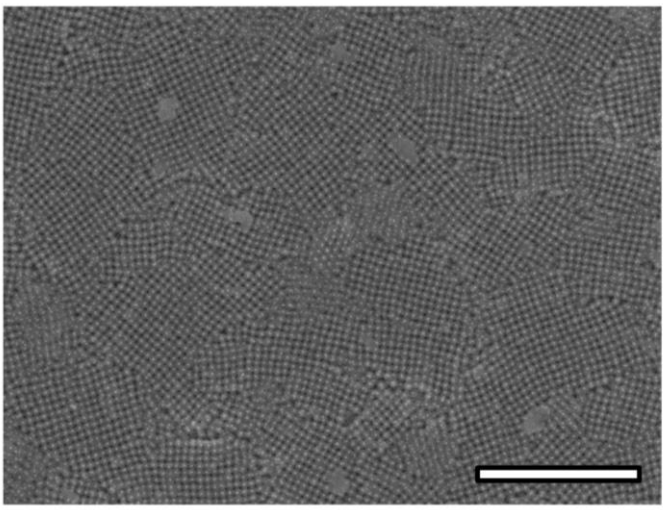

Figure S9: Polycrystalline 5-layer thin film grown on an unpatterned substrate. Scale bar is 1 μm.